these two reactions suggests that the products $CH_2(\tilde{a}) + N_2(X)$ should be favored in the reaction of NH(a) with HCN, which, however, were not observed.

Registry No. NH, 13774-92-0; NO, 10102-43-9; HCN, 74-90-8.

Kinetic Study of the Reaction K + O₂ + M (M = N₂, He) from 250 to 1103 K

John M. C. Plane,* B. Rajasekhar,

Rosenstiel School of Marine and Atmospheric Science, University of Miami, 4600 Rickenbacker Causeway, Miami, Florida 33149

and Libero Bartolotti

Department of Chemistry, University of Miami, Coral Gables, Florida 33124 (Received: October 9, 1989; In Final Form: December 1, 1989)

The recombination reaction K + O₂ + M was studied by the technique of pulsed photolysis of a K atom precursor followed by time-resolved laser induced fluorescence spectroscopy of K atoms at λ = 404 or 760 nm. Termolecular behavior was demonstrated and absolute third-order rate constants obtained over the temperature range 250–1103 K. A fit of this data to the form AT^{-n} yields $k(T,M = N_2) = [(8.00 \pm 1.74) \times 10^{-30}](T/300)^{-(1.32\pm0.04)}$ cm⁶ molecule⁻² s⁻¹ and $k(T,M = He) = [(4.51 \pm 0.46) \times 10^{-30}](T/300)^{-(1.22\pm0.07)}$ cm⁶ molecule⁻² s⁻¹. These results are compared to two previous studies of these reactions by different experimental methods, which were in marked disagreement below 600 K. A lower limit of $D_0(K-O_2) > 203$ kJ mol⁻¹ is derived. The rate coefficients are then extrapolated from the experimental temperature range to ambient mesospheric temperatures (140 K < T < 240 K) and to flame temperatures (1500 K < T < 2200 K), by means of the Troe formalism. Finally, the rates of formation and bond energies of LiO₂, NaO₂, and KO₂ are compared.

Introduction

The recombination reaction between potassium atoms and oxygen to form the superoxide

$$K + O_2 + M \rightarrow KO_2 + M \text{ (M = third body)} \quad (1)$$

is of both theoretical and practical interest. The reaction involves the association of two neutral fragments to form KO_2, which is known from matrix isolation studies[1] to exist predominantly as an ion pair, $K^+(O_2)^-$. Reaction 1 thus involves a crossing from a long-range covalent attractive surface onto a close-range ionic potential surface at a K–O₂ separation of 3.7 Å.[2] This type of covalent/ionic curve crossing, together with the relatively high densities of vibrational states characterizing ionic molecules, has the effect of dramatically enhancing the rates of recombination reactions between alkali-metal atoms and species such as OH,[3] I,[4] and O₂.[5-8]

A primary motivation for the present work is to gain an understanding of the chemistry of the alkali metals in the mesosphere, as in the case of our recent studies of the reactions Li + O₂ +

M[7] and Na + O₂ + N₂.[8] These metals are believed to ablate from meteorites on the edge of the Earth's atmosphere,[9] where a layer of the free metal atoms has been observed a few kilometers wide at an altitude of about 90 km.[10] A number of recent atmospheric models[11,12] have indicated that the principal sinks for the metals immediately beneath these layers are their superoxides, formed by recombination reactions with O₂. Of particular interest is to understand the different seasonal behavior of the three metals, particularly striking at high latitudes where the mesosphere undergoes a substantial cooling in summer to about 140 K, compared to 230 K in winter.[13] The column density of atomic Li shows about a 10-fold wintertime enhancement, compared to a 3-fold enhancement for Na and essentially no change for K.[14] Termolecular reactions such as reaction 1 will be sensitive not only to temperature changes but also to the changes in atmospheric pressure that accompany these large seasonal temperature differences.[12] Thus, the measurement of k_1 below 300 K, and a comparison with the temperature dependences for the analogous reactions of Na and Li,[7,8] is of primary importance for understanding the seasonal variations in the mesospheric chemistry of these metals.

In addition, the accurate measurement of k_1 above 1000 K is required to model the combustion of K in oxygen-rich flames.[15] Recent measurements[6,16,17] of k_1 have indicated that reaction 1 is sufficiently rapid at high temperatures that large fluxes of the superoxide will occur in oxygen-rich flames.

(1) Andrews, L. *J. Phys. Chem.* **1969**, *73*, 3922; *J. Chem. Phys.* **1971**, *54*, 4935. Smardzewski, R. R.; Andrews, L. *J. Chem. Phys.* **1972**, *57*, 1327. Jacox, M. E.; Milligan, D. E. *Chem. Phys. Lett.* **1972**, *14*, 518. Huber, H.; Ozin, G. A. *J. Mol. Spectrosc.* **1972**, *41*, 595. Adrian, F. J.; Andrews, L. *J. Phys. Chem.* **1973**, *77*, 801. Andrews, L.; Hwang, J.-T.; Trindle, C. *Ibid.* **1973**, *77*, 1065. Cochran, E. L.; Bowers, V. A. *J. Chem. Phys.* **1973**, *59*, 56; *Chem. Phys. Lett.* **1974**, *25*, 175. Andrews, L. *J. Mol. Spectrosc.* **1976**, *61*, 337. Lindsay, D. M.; Herschbach, D. R.; Kwiram, A. L. *J. Phys. Chem.* **1983**, *87*, 2113.
(2) Grice, R.; Herschbach, D. R. *Mol. Phys.* **1974**, *27*, 159.
(3) Husain, D.; Plane, J. M. C.; Chen, C. X. *J. Chem. Soc., Faraday Trans. 2* **1984**, *80*, 1465 and 1619; *Ibid.* **1985**, *81*, 561 and 769.
(4) Husain, D.; Plane, J. M. C.; Chen, C. X. *J. Chem. Soc., Faraday Trans. 2* **1985**, *81*, 1675. Plane, J. M. C.; Husain, D. *J. Phys. Chem.* **1986**, *90*, 501. Plane, J. M. C.; Husain, D. *J. Chem. Soc., Faraday Trans. 2* **1986**, *82*, 897.
(5) Husain, D.; Plane, J. M. C. *J. Chem. Soc., Faraday Trans. 2* **1982**, *78*, 163. Husain, D.; Marshall, P.; Plane, J. M. C. *Ibid.* **1985**, *81*, 301; *J. Photochem.* **1986**, *32*, 1.
(6) Husain, D.; Plane, J. M. C. *J. Chem. Soc., Faraday Trans. 2* **1982**, *78*, 1175.
(7) Plane, J. M. C.; Rajasekhar, B. *J. Phys. Chem.* **1988**, *92*, 3884.
(8) Plane, J. M. C.; Rajasekahr, B. *J. Phys. Chem.* **1989**, *93*, 3135.

(9) Goldberg, R. A.; Aikin, A. C. *Science* **1973**, *180*, 294.
(10) Megie, G.; Bos, F.; Blamont, J. E.; Chanin, M. L. *Planet. Space Sci.* **1978**, *26*, 27.
(11) Thomas, L.; Isherwood, M. C.; Bowman, M. R. *J. Atmos. Terr. Phys.* **1983**, *45*, 587.
(12) Swider, W. *J. Geophys. Res.* **1987**, *92*, 5621.
(13) Gardner, C. A.; Senft, D. C.; Kwon, K. H. *Nature* **1988**, *322*, 142.
(14) Kvifte, G. *Physics and Chemistry of Upper Atmospheres*; McCormac, B. M., Ed.; Reidel: Dordrecht, Holland, 1973.
(15) Jensen, D. E. *J. Chem. Soc., Faraday Trans. 1* **1982**, *78*, 2835.
(16) Silver, J. A.; Zahniser, M. S.; Stanton, A. C.; Kolb, C. E. *Proceedings of the 20th Symposium (International) on Combustion*; The Combustion Institute: Pittsburgh, PA, 1984; p 605.
(17) Husain, D.; Lee, Y. H.; Marshall, P. *Combust. Flame* **1987**, *68*, 143.

Reaction 1 was first studied directly by Husain and Plane[6] over the temperature range 780–884 K using the technique of flash photolysis with detection of K by time-resolved resonance absorption spectroscopy. This technique was later extended[17] to cover the temperature range from 680 to 1010 K. Silver et al.[16] employed a fast flow tube with laser induced fluorescence (LIF) detection of K to measure k_1 from 302 to 720 K. The measured values of k_1 from these studies are in good agreement in their overlapping temperature range around 700 K. However, Husain et al.[17] obtained a temperature dependence of $T^{-2.6}$ compared with one of $T^{-0.56}$ by Silver et al.[16] Thus, the values of k_1 extrapolated from the two studies[16,17] to mesospheric temperatures (200 K) or flame temperatures (2000 K) disagree by more than an order of magnitude at both temperature extremes. Hence, an important objective of this study, where a different experimental technique is employed, is to measure k_1 over a substantial temperature range in an attempt to resolve the differences between these recent investigations.[16,17]

Experimental Section

Reaction 1 was investigated by time-resolved laser induced fluorescence spectroscopy of K atoms following the pulsed photolysis of a potassium salt vapor in an excess of O_2 and the bath gas (N_2 or He). The experimental system has been described in detail elsewhere.[7,18] Briefly, the reaction was studied in a stainless steel reactor consisting of a central cylindrical reaction chamber at the intersection of two sets of horizontal arms that cross orthogonally. These arms provide the optical coupling of the lasers and the flash lamp to the central chamber where the reaction is initiated, as well as the means by which the flows of the reagent and the bath gas enter the chamber. One of these arms was independently heated to act as a heat-pipe source of the potassium-salt vapor. A fifth vertical side arm provides the coupling for the photomultiplier tube (Thorn EMI Gencom Inc., Model 9816QB) which monitors the LIF signal. The central chamber is enclosed in a furnace which can heat it to over 1100 K. Alternatively, the furnace can be filled with powdered "dry ice" to cool the chamber to below 250 K. The temperature of the gas in the chamber is monitored by a permanently inserted Chromel/Alumel thermocouple whose tip is about 1 cm below the paths of the photolysis and probe lasers in the center of the chamber. This thermocouple is enclosed in an Inconel sheath. Once the selected temperature is reached, the temperature controller (Omega Model 6100) maintains the gas temperature to within 5 K. It was established that the measured temperature was not a function of the mass-flow rate or total pressure of gas in the reactor under the range of conditions used in these experiments, implying rapid thermal equilibration between the gas and the reactor walls. Reaction 1 was studied over the temperature range 250–1103 K using N_2 as the bath gas and from 333 to 1056 K with He.

The potassium atom precursor used for most experiments was potassium acetate. The powdered salt was placed in a tantalum boat in the heat pipe and then carefully heated to about 600 K. At this temperature the acetate sublimated readily, and was then entrained in a flow of the bath gas and carried into the central chamber. The temperature in the heat pipe required careful control because at higher temperatures the decomposition of the acetate in the boat, leaving a carbon residue, became inconveniently rapid. Following the original work of Edelstein and Davidovits,[19] we also employed KI as a precursor for a limited set of experiments above 1000 K and below 400 K and obtained excellent agreement with the kinetic measurements made using CH_3COOK. In addition, the first-order kinetic decays of atomic K were shown to be independent of the residence (or turnover) time of the gas in the reactor. These observations implied that the presence of any carbon residue from the decomposition of CH_3COOK on the walls of the central chamber did not significantly remove O_2. The major advantages of CH_3COOK over KI

(18) Plane, J. M. C. *J. Phys. Chem.* **1987**, *91*, 6552.
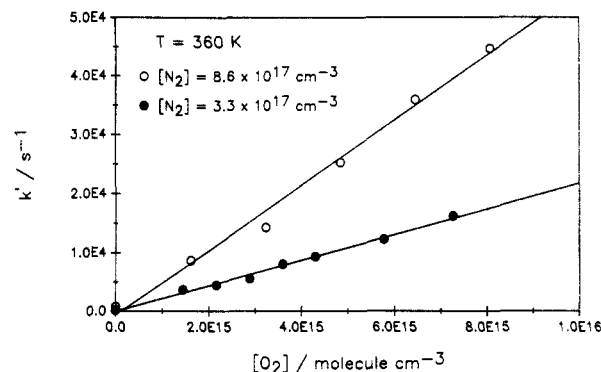(19) Edelstein, S. A.; Davidovits, P. *J. Chem. Phys.* **1971**, *55*, 5164.

Figure 1. Plots of k' against $[O_2]$ at constant $[N_2]$, for $T = 360$ K. The solid lines are linear regression curves through the data.

is that k_1 could be measured between 400 and 800 K without the kinetic interference from I_2 which is formed from the reaction between O_2 and the alkali-metal iodide on the hot walls of the reactor.[7,8] The potassium salt vapor was photolyzed using an excimer laser at 193 nm (Questek, Model 2110, pulse fluence $\approx$ 5 mJ cm^{-2}) or a small flash lamp (EG&G, Model FX193U).[17]

The K atoms were selectively pumped at $\lambda = 404.4$ nm (K-$(5^2P_{3/2})$–K$(4^2S_{1/2})$) by use of a nitrogen-pumped dye laser (Laser Science Inc., Model VSL-337; laser dye DPS, bandwidth $\approx$ 0.01 nm). In experiments below 900 K, when blackbody radiation from the reactor walls was not significant, nonresonant fluorescence was measured at $k = 766.5$ and 769.9 nm (K$(4^2P_{3/2,1/2})$–K$(4^2S_{1/2})$) after passing through an interference filter centered at 768 nm (Edmund Scientific, fwhm = 10 nm). This procedure greatly improved the detection sensitivity by virtually eliminating scattered light. Above 900 K, resonant fluorescence at $\lambda = 404.4$ and 404.7 nm (K$(5^2P_{3/2,1/2})$–K$(4^2S_{1/2})$) was employed after passing through an interference filter centered at 404 nm (Oriel, fwhm = 10 nm). The excimer and dye lasers were arranged to be collinear with the dye laser protected from the excimer beam by a dichroic filter (Newport Corp., Model 10QM20HL1). The diameter of the dye laser was carefully maintained to be $\approx$80% that of the excimer using a beam expander and iris.

Materials. Oxygen (99.995%; Liquid Carbonic) was trapped at 77 K before use. Nitrogen (99.9995%; Liquid Carbonic) and helium (99.9999%; Matheson, "Matheson Purity") were used without further purification. KI (Aldrich; anhydrous 99% purity) was refluxed in the heat pipe at 700–850 K for several hours prior to kinetic experiments to remove traces of I_2. CH_3COOK (Aldrich, anhydrous 99+% purity) was heated to 400 K in the heat pipe and degassed for several hours prior to experiments.

Results

This study was carried out with the K atoms in an excess of O_2 and M (M = N_2 or He), so that the pseudo-first-order decay coefficient k' is given by

$$k' = k_{diff} + k_1[O_2][M] \qquad (2)$$

Figure 1 is a plot of k' against $[O_2]$ at $T = 360$ K, demonstrating a linear dependence on $[O_2]$ and a dependence on $[N_2]$. Note that k_{diff} is of the order of 300–700 s^{-1}, so that this term is negligible compared to the contribution to k' from chemical reaction, and the plots appear to pass through the origin. Figure 2 illustrates plots of $(k' - k_{diff})/[N_2]$ against $[O_2]$ for some of the temperatures at which reaction 1 was studied. Inspection of eq 2 indicates that such plots should be linear with slopes giving $k_1(T)$. Since the sets of points at most of the temperatures illustrated in Figure 2 were measured over a range of pressure (Table I), this figure also demonstrates that reaction 1 is directly proportional to the concentration of the third body. Note that within experimental error the intercepts pass through the origin, in accord with the simple kinetic nature of the system described by eq 2. Table I lists the measured values of k_1 as a function of temperature and bath gas. The quoted errors represent the expected 2σ errors from the linear regression fits to each plot. Included in Table I is the
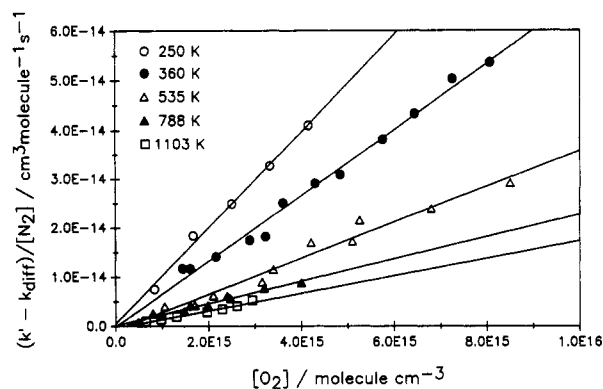
Figure 2. Plots of $(k' - k_{diff})/[N_2]$ against $[O_2]$ for over the temperature range 250–1103 K. The solid lines are linear regression curves through the data.

TABLE I: Experimental Determinations of k_1(K+O_2+N_2) and k_1(K+O_2+He) as a Function of T (Quoted Uncertainty, 2σ)

T/K	$k_1/10^{-30}$ cm^6 molecule^{-2} s^{-1}	press. range/Torr
	K + O_2 + N_2	
250	9.80 ± 0.37	9.3
293	8.20 ± 0.82	9.3
307	7.84 ± 0.69	16.7
360	6.60 ± 0.21	12.2–32.2
433	5.04 ± 0.32	19.7
470	4.32 ± 0.21	19.5
533	3.83 ± 0.44	19.2–31.0
601	3.46 ± 0.10	11.2
615	2.69 ± 0.21	19.0
713	2.36 ± 0.21	18.5–30.0
788	2.21 ± 0.10	18.5–30.0
832	2.1 ± 0.07	19.8
906	1.82 ± 0.15	24.3
988	1.67 ± 0.15	48.0
1103	1.51 ± 0.20	20.5
	K + O_2 + He	
333	4.20 ± 0.70	9.8
481	2.12 ± 0.1	50.0
568	2.05 ± 0.05	36.8
621	1.71 ± 0.05	49.8
683	1.79 ± 0.02	20.8
718	1.86 ± 0.22	26.0
771	1.44 ± 0.03	100.0
791	1.42 ± 0.10	26.0
800	1.21 ± 0.08	35.0
870	1.32 ± 0.09	48.4–74.1
922	1.17 ± 0.46	50.0
1056	0.88 ± 0.08	50.0–75.0

pressure range (Torr) over which measurements were carried out at a particular temperature.

Figure 3 displays the data contained in Table I, plotted as ln (k) vs ln (T). A linear regression fit weighted by uncertainties in Table I yields

$k_1(T, M = N_2) =$

$[(8.00 ± 1.74) \times 10^{-30}](T/300)^{-(1.32±0.04)}$ cm^6 molecule^{-2} s^{-1}

$$(3)$$

$k_1(T, M = He) =$

$[(4.51 ± 0.46) \times 10^{-30}](T/300)^{-(1.22±0.07)}$ cm^6 molecule^{-2} s^{-1}

$$(4)$$

where the quoted confidence limits are the expected 2σ uncer-

Figure 3. Plots of ln (k_1) against ln (T) for M = N_2 and He. The solid lines are weighted linear regression curves through the sets of experimental data for each third body.

Figure 4. Plots of all experimental data on the reactions K + O_2 + M (M = N_2, He). Solid lines illustrate the best fit to the present data. The results of the two other temperature-dependent studies (refs 16 and 17) are summarized by plotting their recommended expressions for $k_1(T)$ over the experimental temperature range in each case.

tainties calculated from the absolute errors in Table I.

Discussion

The results of the present study of k_1 are compared with the previous studies[6,16,17] in Figure 4. Table II lists the values of k_1(M = N_2, T = 300, 700, 1000 K) calculated from the temperature dependences given in the previous studies[16,17] and expression 3. We are in reasonable agreement with the original study of Husain and Plane[6] for M = N_2 and He and in good agreement with Husain et al.[17] over the overlapping range of temperature from 680 to 1010 K for M = N_2. However, the $T^{-2.6}$ dependence obtained in that study[17] is considerably greater than the $T^{-1.3}$ dependence in the present study. We postulated previously, when discussing a similar discrepency for the reaction Na + O_2 + N_2,[8] that the production of I_2 from the heterogeneous reaction between O_2 and adsorbed NaI in the quartz reaction cell used by Husain et al.[17] might be responsible for their larger T dependence. If the same kinetic interference was present in their study of reaction 1,[17] it would have been more pronounced at lower temperatures where the equilibrium between I_2 and I is on the molecular side. Indeed, if their data for temperatures only above 700 K is considered, then a $T^{-1.8}$ dependence is obtained, in better accord with the present result.

The rate coefficients determined by Silver et al.[16] are not in agreement with the present study except for k_1(700 K,M = N_2). For example, their results are 33% and 52% slower for M = N_2 and He, respectively, at 300 K. We observed the same discrepancy

TABLE II: Comparison of Measured Rate Coefficients for the Reaction K + O_2 + N_2

reference	method[a]	T range/K	k_1(300 K)[b]/cm^6 molecule^{-2} s^{-1}	k_1(700 K)[b]/cm^6 molecule^{-2} s^{-1}	k_1(1000 K)[b]/cm^6 molecule^{-2} s^{-1}
this work	FP-LIF	250–1103	$(8.0 ± 1.7) \times 10^{-30}$	$(2.6 ± 0.6) \times 10^{-30}$	$(1.6 ± 0.4) \times 10^{-31}$
Silver et al.[19]	FT-LIF	320–700	$(5.4 ± 0.2) \times 10^{-30}$	$(3.4 ± 0.6) \times 10^{-30}$	$(2.8 ± 0.6) \times 10^{-31}$
Husain et al.[17]	FP-RA	688–1016	$(24 ± 19) \times 10^{-30}$	$(2.6 ± 2.3) \times 10^{-30}$	$(1.1 ± 0.9) \times 10^{-31}$

[a] FP, flash photolysis; LIF, laser-induced fluorescence; RA, resonance absorption; FT, flow tube; RF, resonance fluorescence. [b] Calculated from the recommended k_1(T) given in each study.
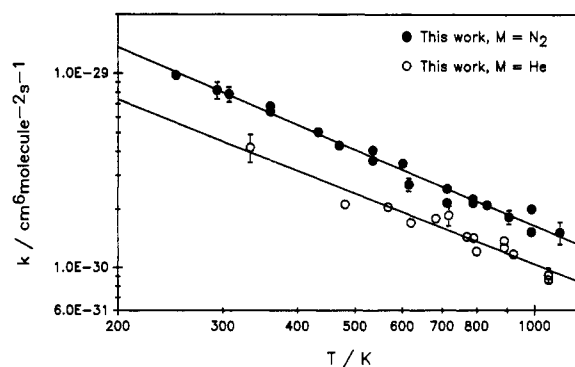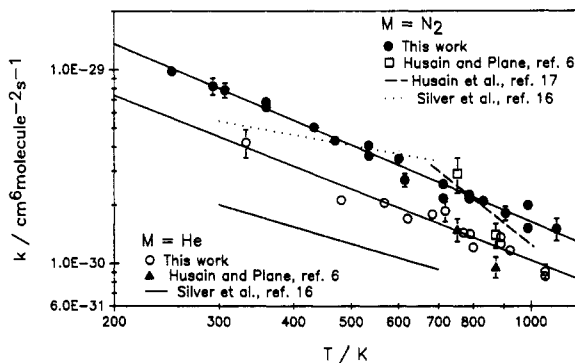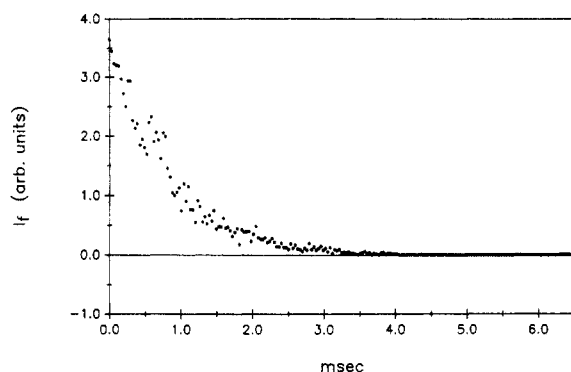
Figure 5. Time-resolved decay of LIF signal from K atoms at $\lambda = 404$ nm $(K(5^2P_J) - K(4^2S_{1/2}))$ following pulsed photolysis of KI vapor at 1056 K: $[O_2] = 3.75 \times 10^{15}$ cm^{-3}; $[He] = 6.8 \times 10^{17}$ cm^{-3}.

TABLE III: Derivation of the Experimental Bond Dissociation Energy of KO_2

$[O_2]/$ 10^{16} molecules cm^{-3}	k_{diff}/k'	$K_{eq}^a/$ 10^{-14} cm^3 molecule^{-1}	$D_0^a/$ kJ mol^{-1}
0.38	0.45	3.85	207
1.13	0.28	2.18	202
1.50	0.12	2.58	203

^{a} Lower limit; see text for discussion of diffusion corrections.

TABLE IV: Comparison of ab Initio and Experimental Geometries of KO_2 and O_2^-

	$r_{K-O}/$Å	$\Delta\%^a$	$r_{O-O}/$Å	$\Delta\%^a$
experiment[1]	2.28		1.28	
UHF/GEN^b	2.55	11.8	1.35	5.5
UHF/GEN(d)^c	2.44	7.0	1.29	0.8
O_2^-				
experiment[32]			1.33	
UHF/GEN			1.35	1.5
UHF/GEN(d)			1.29	3.0

^{a} Percentage difference from the experimental value. ^{b} UHF, unrestricted Hartree–Fock calculation; GEN, augmented basis sets excluding d functions (see Appendix). ^{c} GEN(d), augmented basis sets including d functions (see Appendix).

for the reaction $Na + O_2 + N_2$.[8] In the case of the Na reaction a systematic error in the flow-tube experiment was reported for $M = N_2$,[16] although not for $M = He$ where we were in agreement.[8] The reasons for the present discrepancy, especially for $M = He$, are unknown. However, the $T^{-0.56}$ dependence for $k_1(T,M = N_2)$ seems to be rather small compared to the $T^{-0.9}$ dependence for $k_1(T,M = He)$ measured by Silver et al.,[16] although the experimental errors are large. Usually, the more efficient third body has a steeper T dependence reflecting the tendency for third bodies to display increasingly similar efficiencies at elevated temperatures.[20]

We now describe an extrapolation of $k_1(T)$ from the measured temperature range of 250–1103 K to temperature regimes characteristic of the mesosphere and of combustion processes.

Extrapolation of $k_1(K+O_2+M)$ from 140 to 2200 K. For the purpose of this calculation, we assume that reaction 1 goes primarily by the energy-transfer mechanism.[7,8] It is also necessary to establish that the experimental measurements of $k_1(T)$ in this study are close to the rate coefficient at the low-pressure limit, $k_{rec,0}$. We have followed the procedure described in our previous papers,[7,8] based on the work of Luther and Troe.[21] The calculation requires an estimate of the high-pressure rate constant, $k_{rec,\infty}$, which is calculated in terms of the orbiting criteria on the attractive surface due to the long-range van der Waals interaction between K and O_2.[7,8,22] The dispersion coefficient $C_6 = 1.40 \times 10^7$ J mol^{-1} Å^6 is calculated from the Slater–Kirkwood formula[23] using the polarizabilities of K and O_2 from refs 24 and 25, respectively. Over the temperature range of the present study, this yields $k_{rec,\infty}(250$ K) $= 5.56 \times 10^{-10}$ cm^3 molecule^{-1} s^{-1} and $k_{rec,\infty}(1103$ K) $= 7.12 \times 10^{-10}$ cm^3 molecule^{-1} s^{-1}. This calculation indicates that at the pressure of 9.3 Torr of N_2, at which we measured k_1 at 250 K, $k_1/k_{rec,0} = 0.90$; at 1103 K and 20.5 Torr of N_2, $k_1/k_{rec,0} = 0.95$. Thus, our experiments are essentially at the low-pressure limit.

In order to carry out a temperature extrapolation of $k_1(T)$, we employ the formalism of Troe which is based on a simplified solution of RRKM theory.[26] We have described in detail elsewhere[3,5,7,8] the application of this formalism to such a set of experimental measurements. An important parameter that is required for these calculations is the bond energy of KO_2, $D_0(K-O_2)$. This quantity is poorly known from work on K seeded into oxygen-rich flames,[15] and in the following section we describe an experimental and theoretical determination of the superoxide bond energy.

Determination of $D_0(K-O_2)$. The experimental estimate of $D_0(K-O_2)$ was obtained from the kinetic data according to a procedure we have described fully elsewhere.[27] Figure 5 illustrates an example of the time-resolved decay of the LIF signal at $\lambda = 404$ nm, generated by the pulsed photolysis of KI in an excess of O_2 and He at 1056 K. The signal-to-noise of this decay is more than 200:1. There is no evidence of the decay of atomic K in Figure 5 approaching an equilibrium above the base line. Thus, this decay can be used to derive a lower limit for the equilibrium constant K_{eq} for reaction 1 at 1056 K, assuming that the superoxide molecules do not undergo further reaction.[27] The lower limit to $D_0(K-O_2)$ is then extracted from a statistical mechanical calculation of K_{eq}, using the experimental geometries and vibrational frequencies[1] in the partition functions. The results of analyzing three such decays are listed in Table III. The contribution of k_{diff} to k' (eq 2) has to be accounted for, particularly when the contributions to k' from chemical reaction and diffusion are of similar size: in that case, $D_0(K-O_2)$ will be overestimated when $[O_2]$ is small. This effect is illustrated in Table III, where the O_2 concentration is varied by about a factor of 5. The best estimate is therefore $D_0(K-O_2) \geq 203$ kJ mol^{-1}.

Following our previous theoretical calculations of $D_0(Li-O_2)$ and $D_0(Na-O_2)$,[27] we performed a limited number of ab initio calculations on KO_2. The major features of the alkali-metal superoxide potential surfaces have been discussed in detail by Alexander.[28] The surfaces contain two minima, corresponding to a linear A–O–O molecule $(C_{\infty v})$ and to an isosceles triangular geometry (C_{2v}). All the theoretical studies[27-31] agree that the absolute energy minimum corresponds to the $^2A_2$ surface in C_{2v} geometry.

Although some covalent character must be present in ground-state KO_2, since the purely ionic and covalent diabatic curves cross at only 3.7 Å,[2] there is strong experimental evidence[1] that the molecule is predominantly ionic. Hence, the energy required to dissociate to the ions is expected to correlate well with the energy of the equilibrium molecular geometry. The overall dissociation energy to K and O_2 is then given by

$$D_0(K-O_2) =$$
$$E(K^+) + E(O_2^-) - E(KO_2) - IP(K) + EA(O_2) + ZPE \quad (5)$$

(20) Endo, H.; Glanzer, K.; Troe, J. *J. Phys. Chem.* **1979**, *83*, 2083.

(21) Luther, K.; Troe, J. *Proceedings of the 17th Symposium (International) on Combustion*; The Combustion Institute: Pittsburgh, PA, 1978; p 535.

(22) Smith, I. W. M. *Kinetics and Dynamics of Elementary Gas Reactions*; Butterworths: London, 1980.

(23) Slater, J. C.; Kirkwood, J. G. *Phys. Rev.* **1931**, *37*, 682.

(24) Chamberlain, G. E.; Zorn, J. C. *Phys. Rev.* **1963**, *129*, 677.

(25) Hirschfelder, J. O.; Curtiss, C. F.; Bird, R. B. *Molecular Theory of Gases and Liquids*; Wiley: New York, 1954.

(26) Troe, J. *J. Chem. Phys.* **1977**, *66*, 4745 and 4758; *J. Phys. Chem.* **1979**, *83*, 114.

(27) Plane, J. M. C.; Rajasekhar, B.; Bartolotti, L. *J. Phys. Chem.* **1989**, *93*, 3141.

(28) Alexander, M. H. *J. Chem. Phys.* **1978**, *69*, 3502.

(29) Billingsley, F. P.; Trindle, C. *J. Phys. Chem.* **1972**, *76*, 2995.

(30) O'Neill, S. V.; Schaefer, H. F.; Bender, C. F. *J. Chem. Phys.* **1973**, *59*, 3608.

(31) Grow, D. T.; Pitzer, R. M. *J. Chem. Phys.* **1977**, *67*, 4019.

TABLE V: Ab Initio Calculations of the Mulliken Electron Populations and Dipole Moments of KO$_2$

	q_A	q_O	μ_D/D
UHF/GEN	0.944	−0.472	10.8
UHF/GEN(d)	0.884	−0.442	9.08

where $E(\ )$ indicates the absolute electronic energy; IP(K) is the ionization potential of potassium and EA(O$_2$) is the electron affinity of oxygen, both of which are accurately known from experiment;[32] ZPE is the difference between the zero-point vibrational energies of O$_2^-$ and KO$_2$. For eq 5 to produce accurate bond energies, the basis sets should at least approach the Hartree–Fock (HF) limit. We have therefore employed the greatly augmented basis sets developed by Bauschlicher et al.[33] for determining the bond energies of molecules containing metal atoms. However, because of limited computer resources, we did not include f functions or make corrections for electron correlation. The details of the basis sets are given in the Appendix.

The equilibrium geometry of KO$_2$ was first calculated from an unrestricted Hartree–Fock (UHF) SCF optimization, using the Gaussian 86 program.[34] This calculation determined that the ground state of the molecule is $^2A_2$ in C_{2v} symmetry. Calculations were also performed by using the augmented basis set but without d functions. Table IV compares the UHF equilibrium geometries using these basis sets with the experimental geometries for KO$_2$ and O$_2^-$.[1,32] There is clearly much better agreement with experiment when the d functions are added to the basis sets, as expected because of the increased flexibility of the representation. The Mulliken charge distribution and the dipole moment of KO$_2$ are listed in Table V, confirming its highly ionic nature.[1] Note that the addition of d functions increases the polarizability of the atomic wave functions, enabling a redistribution of charge from the metal center back to the oxygen atoms and considerably shortening the K–O bond distance. The bond energy calculation is illustrated in Table VI. As expected, when d functions are added, the bond energy increases considerably. However, the calculated value is still 49 kJ mol^{-1} below our experimental lower limit. Some of this difference would be made up if electron correlation was included: in the case of D_0(Li–O$_2$) and D_0(Na–O$_2$) we found that the correction for electron correlation, computed at the MP4 level,[34] amounted to a 16–30 kJ mol^{-1} increase in bond energy.[27] In addition, the inclusion of f functions would probably lead to a slightly shorter K–O bond and a modest increase in the bond energy. The important point is that these corrections should not increase D_0(K–O$_2$) much above the experimental lower limit, which is thus probably close to the actual bond energy. We therefore use D_0(K–O$_2$) = 203 kJ mol^{-1} in the calculations that follow.

Further Data Input for Application of the Troe Formalism.[26] The parameters used in the calculations are listed in Table VII. The choice of parameters is discussed below.

1. Lennard-Jones Parameters. σ(KO$_2$–M) and ϵ(KO$_2$–M) have to be assumed in order to calculate the Lennard-Jones collision frequency between KO$_2$ and M (N$_2$ or He). Fortunately the calculation is not very sensitive to these parameters, and their choice is based on our previous studies.[7,8]

2. Fundamental Frequencies and Geometry of KO$_2$. The bond lengths and vibrational frequencies listed in Table VII are taken from the study by Andrews and co-workers[1] of KO$_2$ in an inert gas matrix and are assumed to be unchanged in the gas phase. The vibrational frequency ν_3 corresponds to the O$_2^-$ stretching frequency.

Figure 6. Plots illustrating fitting of Troe formalism to present experimental data for K + O$_2$ + M (M = N$_2$, He). The solid lines are an extrapolation over the temperature range 140–2200 K.

Figure 7. Plots of experimental data from the present study and refs 7 and 8 for the reactions Li, Na, and K + O$_2$ + N$_2$ over the temperature range 230–1118 K.

The results of applying the Troe formalism[26] to reaction 1 are listed in Table VII for M = N$_2$ and He at 300 K. The collision efficiencies β_c(N$_2$) = 0.30 and β_c(He) = 0.12 are obtained by comparing the calculated strong collision rate coefficient, $k_{rec,0}^{sc}$, with the result for k_1(300 K) from the best fit to the experimental data given in expressions 3 and 4. The values of β_c and $\langle \Delta E \rangle$ (the average energy transferred upon collision between KO$_2$ and M) are in accord with a wide body of data of the collision efficiencies of this third body.[5,7,8,21,35]

The fit of the Troe formalism to the experimental data at 300 K can now be used to calculate $k_{rec,0}$ over the temperature range of the present study and then to compare with the experimental values of $k_1(T)$. The best fit to the set of experimental data is obtained by assuming small positive temperature dependences for $\langle \Delta E \rangle$ (see Table VIII), in accord with recent work on collisional energy transfer from vibrationally excited CS$_2$.[36] These calculations are illustrated in Figure 6 and are seen to be highly satisfactory. Patrick and Golden[37] have previously calculated k_1(200 K < T < 2000 K, M = N$_2$) using the Troe formalism.[26] They fitted their calculation to the measured k_1 of Silver et al.[16] at 302 K and assumed a temperature dependence for $\langle \Delta E \rangle \propto T^{0.0}$, so that their calculation is more than 50% below the present result.

$k_1(T)$ can now be extrapolated outside the experimental temperature range of the present study. This is illustrated in Figure 6 from 140 to 2000 K. The recommended result for k_1-(K+O$_2$+N$_2$) in the temperature region of interest for modeling the mesospheric chemistry of K is given by

$$k_1(140 \text{ K} < T < 240 \text{ K}) =$$
$$(1.3 \times 10^{-29})(T/200 \text{ K})^{-1.23} \text{ cm}^6 \text{ molecule}^{-2} \text{ s}^{-1}$$

The extrapolation of k_1 to flame temperatures yields

$$k_1(1500 < T < 2200 \text{ K}) =$$
$$(4.0 \times 10^{-31})(T/2000 \text{ K})^{-1.96} \text{ cm}^6 \text{ molecule}^{-2} \text{ s}^{-1}$$

(32) JANAF Thermochemical Tables, 3rd ed.; Chase, M. W., Jr., Davies, C. A., Downey, J. R. Jr., Frurip, D. J., McDonald, R. A., Syverud, A. N., Eds.; *J. Phys. Chem. Ref. Data* **1985**, *14*.

(33) Bauschlicher, C. W. Jr.; Langhoff, S. R.; Partridge, H. *J. Chem. Phys.* **1986**, *84*, 901.

(34) Frisch, M. J.; Binkley, J. S.; Schlegel, H. B.; Raghavachari, K.; Melius, C. F.; Martin, R. L.; Stewart, J. J. P.; Bobrowicz, F. W.; Rohlfing, C. M.; Kahn, L. R.; Defrees, D. J.; Seeger, R.; Whiteside, R. A.; Fox, D. J.; Fleuder, E. M.; Pople, J. A. *Gaussian 86*; Carnegie-Mellon Quantum Chemistry Publishing Unit: Pittsburgh, PA, 1984.
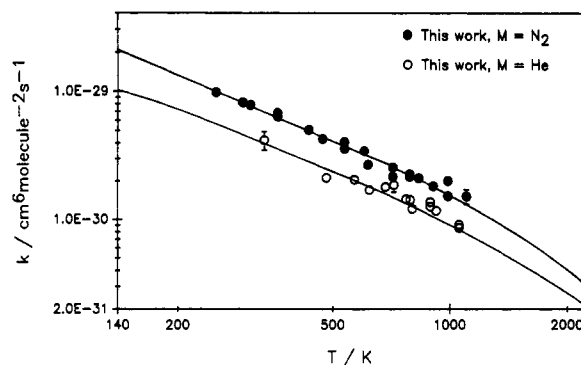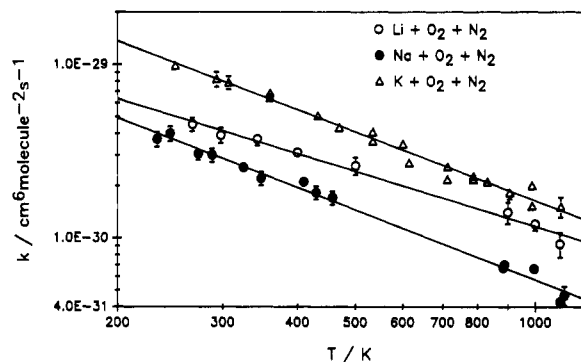
(35) Heymann, M.; Hippler, H.; Troe, J. *J. Chem. Phys.* **1984**, *80*, 1853.

(36) Heymann, M.; Hippler, H.; Plach, H. J.; Troe, J. *J. Chem. Phys.* **1987**, *87*, 3867.

(37) Patrick, R.; Golden, D. M. *Int. J. Chem. Kinet.* **1984**, *16*, 1567.

TABLE VI: Calculation of ab Initio Bond Dissociation Energy

	$E(KO_2)^a$	$E(K^+)^a$	$E(O_2^-)^a$	$D_e(KO_2 \rightarrow K^+ + O_2^-)^b$	$D_e(K-O_2)^{b,c}$	$D_0(K-O_2)^{b,d}$
UHF/GEN	$-748.789\,082\,3$	$-589.996\,475\,1$	$-149.604\,539\,7$	494.1	117.7	114.0
UHF/GEN(d)	$-748.839\,570\,7$	$-598.996\,475\,1$	$-149.639\,560\,1$	534.4	158.0	154.3

^{a} Units: hartrees. ^{b} Units: kJ mol^{-1}. ^{c} Calculated using IE(K) = 4.34 eV and EA(O$_2$) = 0.44 eV (ref 32). ^{d} Difference in zero-point energies is calculated from ref 1 and ref 32.

TABLE VII: Extrapolation of Rate Data for the Reaction K + O$_2$ + M^a

Input Parameters for the KO$_2$ Molecule

R_{K-O} = 2.28 Å, R_{O-O} = 1.28 Å, I_{ABC} = 1.007 × 10^4 amu^3 Å^6, ν_1 = 300 cm^{-1}, ν_2 = 307.5 cm^{-1}, ν_3 = 1108 cm^{-1}, E_0 = 203 kJ mol^{-1}

Data for K + O$_2$ + N$_2$ at T = 300 K

$\sigma(KO_2-N_2)$ = 5.5 Å, $\epsilon(KO_2-N_2)/k$ = 500 K, Z_{LJ} = 1.1 × 10^{-9} cm^3 molecule^{-1} s^{-1}, K_{eq} = 3.1 × 10^{11} cm^3 molecule^{-1}, E_z = 10.3 kJ mol^{-1}, s = 3, m = 2, r = 0, Q_{vib} = 1.71, a = 0.99, $p(E_0)$ = 0.130, F_E = 1.024, F_{anh} = 1.72, F_{rot} = 54.7, I^+/I = 91.0, C_ν = 0.0026, ν = 1.44, $k_{diss,0}^{sc}$ = 8.62 × 10^{-41} cm^3 molecule^{-1} s^{-1}, $k_{rec,0}^{sc}$ = 2.65 × 10^{-29} cm^6 molecule^{-2} s^{-1}, β_c = 0.30, $\langle\Delta E\rangle$ = -1.7 kJ mol^{-1}

Data for K + O$_2$ + He at T = 300 K

$\sigma(KO_2-He)$ = 4.5 Å, $\epsilon(KO_2-He)/k$ = 450 K, Z_{LJ} = 1.46 × 10^{-9} cm^3 molecule^{-1} s^{-1}, $k_{diss,0}^{sc}$ = 1.20 × 10^{-40} cm^3 molecule^{-1} s^{-1}, $k_{rec,0}^{sc}$ = 3.69 × 10^{-29} cm^6 molecule^{-2} s^{-1}, β_c = 0.12, $\langle\Delta E\rangle$ = -0.48 kJ mol^{-1}

^{a} For the definition of symbols not in the present text see ref 27.

Conclusions

Figure 7 illustrates a comparison between our measurements of the three reactions Li, Na, and K + O$_2$ + N$_2$, demonstrating that the rate coefficients lie in the order K > Li > Na:[7,8]

$k_1(K+O_2+N_2)$ =
  $[(8.00 \pm 1.74) \times 10^{-30}](T/300)^{-(1.32\pm0.04)}$ cm^6 molecule^{-2} s^{-1}

$k(Li+O_2+N_2)$ =
  $[(4.30 \pm 1.36) \times 10^{-30}](T/300)^{-(1.02\pm0.6)}$ cm^6 molecule^{-2} s^{-1}

$k(Na+O_2N_2)$ =
  $[(2.90 \pm 0.71) \times 10^{-30}](T/300)^{-(1.30\pm0.04)}$ cm^6 molecule^{-2} s^{-1}

This can be understood in terms of RRKM theory.[26] The K reaction is fastest because the B$_2$ (asymmetric stretch) and the A$_1$ (symmetric stretch) vibrational frequencies of KO$_2$ are significantly lower than the corresponding frequencies of NaO$_2$ and especially LiO$_2$,[1,7,8] leading to a very high density of vibrational states at the critical energy for KO$_2$. The Li reaction is next because D_0(LiO$_2$) is considerably higher than D_0(NaO$_2$) or D_0-(KO$_2$).[27] Of course, all three reactions are faster than the recombination reactions of atoms such as H or O with O$_2$ by 2–3 orders of magnitude,[38] demonstrating how the ionic nature of the alkali-metal superoxides dramatically enhances their rates of formation.

The three reactions have very similar temperature dependences over the experimental range from 230 to 1120 K. Use of the Troe formalism[7,8,26] indicates that this will continue into the temperature range applicable to the mesosphere (140–240 K). Thus, it must be concluded that differences in the temperature dependences of these reactions are not responsible for the different seasonal behavior of the three metals in the high-latitude mesosphere (see Introduction).

Finally, it should be noted that the bond energies of the alkali-metal superoxides remain rather uncertain, although a consensus has emerged over the past 2 years that they are much more strongly bound than had been concluded hitherto. The situation is summarized in Table VIII, which lists the values for the bond

TABLE VIII: Bond Dissociation Energies of the Alkali-Metal Superoxides

D_0/kJ mol^{-1}	method of calculation	reference
	Li–O$_2$	
222 ± 25	flame study	Dougherty et al.[39]
220	semiempirical estimate	Alexander[28]
302 ± 21	flame study	Steinberg and Schofield[40]
≥180	time-resolved kinetics	Plane et al.[27]
296	ab initio calculation	Plane et al.[27]
259	ab initio calculation	Allen et al.[41]
	Na–O$_2$	
234 ± 13	flame study	McEwan and Phillips[42]
150	semiempirical estimate	Alexander[28]
170 ± 25	flame study	Jensen[15]
≤184	molecular beam study	Figger et al.[43]
146 ± 21	flame study	Hynes et al.[44]
<115	thermochemical measurement	Lamoreaux and Hildenbrand[45]
242 ± 21	flame study	Steinberg and Schofield[40]
≥202	time-resolved kinetics	Plane et al.[27]
186	ab initio calculation	Plane et al.[27]
≥230 ± 5	time-resolved kinetics	Marshall et al.[46]
	K–O$_2$	
170 ± 30	flame study	Jensen[15]
247 ± 21	flame study	Steinberg and Schofield[40]
≥203	time-resolved kinetics	this work
154	ab initio calculation	this work

energies obtained from experiment and theory, in chronological order for each of the metals. The superoxide bond energies derived from the early flame work were incorrect because the recombination reactions such as reaction 1 were thought to be about 3 orders of magnitude slower[47] than was subsequently demonstrated in direct time-resolved experiments.[5-8,16,17,46] However, the most recent bond energies from work on alkali metals in oxygen-rich flames[40] are now in excellent agreement with the lower limits derived from time-resolved kinetic studies.[27,46] In the case of D_0(Li–O$_2$) there is also very good agreement between the recent flame study[40] and our theoretical value.[27] However, the ab initio calculations of D_0(Na–O$_2$) and D_0(K–O$_2$) appear to be about 40 kJ mol^{-1} lower than the experimental values (see Table VIII). Further theoretical study of NaO$_2$ and KO$_2$ is clearly required.

Appendix

The potassium basis set is based on that published recently by Bauschlicher et al.[33] This starts with Wachters' basis set[48] of

(38) DeMore, W. B.; Margitan, J. J.; Molina, M. J.; Watson, R. T.; Golden, D. M.; Hampson, R. F.; Kurylo, M. J.; Howard, C. J.; Ravishankara, A. R. *Chemical Kinetics and Photochemical Data for Use in Stratospheric Modeling*; JPL Publication 85-37; Jet Propulsion Laboratory: Pasadena CA, 1985.

(39) Dougherty, G. J.; McEwan, M. J.; Phillips, L. F. *Combust. Flame* **1973**, *21*, 253.

(40) Steinberg, M.; Schofield, K. The High-Temperature Chemistry and Thermodynamics of Alkali Metals (Lithium, Sodium and Potassium) in Oxygen Rich Flames. Preprint; Western Section, The Combustion Institute, November 1987.

(41) Allen, W. D.; Horner, D. A.; DeKock, R.; Remington, R. B.; Schaefer, H. F. The Lithium Superoxide Radical: Symmetry Breaking Phenomena and Potential Energy Surfaces. Submitted for publication *in Chem. Phys.*

(42) McEwan, M. J.; Phillips, L. F. *Trans. Faraday Soc.* **1966**, *62*, 1717.

(43) Figger, H.; Schrepp, W.; Zhu, X. *J. Chem. Phys.* **1983**, *79*, 1320.

(44) Hynes, A. J.; Steinberg, M.; Schofield, K. *J. Chem. Phys.* **1984**, *80*, 2585.

(45) Lamoreaux, R. H.; Hildenbrand, D. L. *J. Phys. Chem. Ref. Data* **1984**, *13*, 151.

(46) Marshall, P.; Narayan, A. S.; Fontijn, A. Kinetic and *thermochemical* Studies of the Recombination Reaction Na + O$_2$ + N$_2$ from 590 to 1515 K by a Modified High-Temperature Photochemistry Technique. Submitted for publication in *J. Phys. Chem.*

(47) Carabetta, R.; Kaskan, W. E. *J. Phys. Chem.* **1968**, *72*, 2483.

fourteen s functions contracted to eight [150591 (0.00026) + 22629.6 (0.00200) + 5223.16 (0.01015) + 1498.06 (0.04043) + 495.165 (0.12732) + 180.792 (0.29872), 71.1940 (0.41837) + 29.3723 (0.23705), 8.68863 (1.0), 3.46382 (1.0), 0.811307 (1.0), 0.312555 (1.0), 0.035668 (1.0), 0.016517 (1.0)], and nine p functions contracted to four [867.259 (0.00234) + 205.254 (0.01880) + 65.8214 (0.08668), 24.5742 (0.25041) + 9.87704 (0.42972) + 4.11693 (0.35117), 1.55653 (1.0), 0.614068 (0.56842) + 0.228735 (0.32743)].

To this are added one s function [0.111 (1.0)], three p functions [0.1236 (1.0), 0.06261 (1.0), 0.02281 (1.0)], and six d functions contracted to five [6.2167 (0.242602) + 1.9493 (0.841179), 0.75929 (1.0), 0.44548 (1.0), 0.13968 (1.0), 0.05441 + (1.0)]. The final contracted basis set is (15s13p6d/9s7p5d).

The oxygen basis set starts with the set of Poirier et al.:[49] eleven s functions contacted to six [18045.3 (0.00041) + 2660.12 (0.00333) + 585.663 (0.01800) + 160.920 (0.072860) + 51.1637 (0.217960) + 17.8966 (0.424260), 6.63901 (1.0), 2.09625 (1.0), 0.842082 (1.0), 0.307328 (1.0), 0.132539 (1.0)]; seven p functions contracted to four [49.8279 (0.008940) + 11.4887 (0.057680) + 3.60924 (0.192130) + 1.31104 (0.355350), 0.502347 (1.0), 0.195677 (1.0), 0.072412 (1.0)].

Following Bauschlicher and Langhoff,[33] three d functions are added [3.0 (1.0), 1.0 (1.0), 0.3 (1.0)]. Thus the final basis set is 11s7p3d/6s4p3d.

(48) Wachters, A. J. H. *J. Chem. Phys.* **1970**, *52*, 1033.

(49) Poirier, R.; Kari, R.; Csizmadia, I. G. *Handbook of Gaussian Basis Sets: a Compendium for ab Initio Molecular Orbital Calculations*; Elsevier: Amsterdam/New York, 1985.

Photochromism of Spiropyrans in Aluminosilicate Gels

Deborah Preston,[†] Jean-Claude Pouxviel,[‡] Thomas Novinson,[§] William C. Kaska,[⊥] Bruce Dunn,*,[‡] and Jeffrey I. Zink*,[†]

Department of Chemistry and Biochemistry, and Department of Materials Science and Engineering, University of California, Los Angeles, California 90024 (Received: October 31, 1989)

Aluminosilicate sol–gels containing photochromic spiropyran molecules (6-nitro-1′,3′,3′-trimethylspiro[2*H*-1-benzopyran-2,2′-indoline] and its derivatives) were prepared. The photochromism was studied by transient absorption spectroscopy and luminescence spectroscopy. Stable, solid photochromic gels were prepared whose photochromic properties remained constant after an initial aging period. Four stages of the gelation process were observed and proved by the rates and spectra of the encapsulated photochromic molecules. The rate of return of the excited photochromic molecule to the initial state was measured during the various stages of the gelation process.

Introduction

Sol–gel synthesis of inorganic glasses offers a low-temperature route to the microencapsulation of organic and organometallic molecules in inorganic matrices.[1–12] The encapsulated molecule can be used to induce new optical properties in the material (i.e., laser action)[3] or to probe the changes at the molecular level which occur during the polymerization, aging, and drying of the glass. A fascinating group of molecules which can function in both of the above capacities are the photochromic substituted 6-nitro-spiro[2*H*-1-benzopyran-2,2′-indolines), abbreviated as BIPS.[13] The structures of the species before and after illumination are sketched in Figure 1. These new transparent photochromic solids have a variety of potential applications. In addition, variations in the rates of the photochromic reactions probe the changes occurring during gelation as demonstrated by Avnir et al. in silicate gel-glass.[10]

The gel-glass studied here is an aluminosilicate formed by hydrolysis and condensation reactions of the precursor (diisobutoxyalumino)triethoxysilane, $(OBu)_2Al-O-Si(OEt)_3$, called ASE.[14–16] Clear, transparent monoliths having dimensions of the order of 1 × 1 × 1 cm are readily prepared under neutral hydrolysis conditions. The initial sol, which is completely fluid, is transformed into a solid, brittle material. After the addition of water, small particles on the order of 10–20 Å in diameter are formed as a consequence of the hydrolysis of the Al–OR groups

to Al–OH and the condensation of the Al–OH groups into –Al–O–Al– polymers. After this step, a slow aggregation takes place which forms inorganic clusters having a ramified and open structure. Subsequent reactions form –Si–O–Si– linkages.[16]

Prior studies with ASE gels reported the use of luminescent molecules to probe the local chemical and structural changes which occur during the sol-gel process.[1,2] Luminescence from pyranine

[†] Department of Chemistry and Biochemistry.
[‡] Department of Materials Science and Engineering.
[§] Current address: Naval Civil Engineering Laboratory, Port Hueneme, CA 93043.
[⊥] Current address: Department of Chemistry, University of California, Santa Barbara, CA 93106.

(1) McKiernan, J.; Pouxviel, J. C.; Dunn, B.; Zink, J. I. *J. Phys. Chem.* **1989**, *93*, 2129.
(2) Pouxviel, J. C.; Dunn, B.; Zink, J. I. *J. Phys. Chem.* **1989**, *93*, 2134.
(3) Dunn, B. D.; Knobbe, E.; McKiernan, J.; Pouxviel, J. C.; Zink, J. I. In *Better Ceramics Through Chemistry III*; Brinker, C. J., Clark, D. E., Ulrich, D. R., Eds.; MRS Symp. Proc. Vol. 121; Materials Research Society: Pittsburgh, 1988; pp 331–342.
(4) Avnir, D.; Levy, D.; Reisfeld, R. *J. Phys. Chem.* **1984**, *88*, 5956.
(5) Levy, D.; Reisfeld, R.; Avnir, D. *Chem. Phys. Lett.* **1984**, *109*, 593.
(6) Avnir, D.; Kaufman, V.; Reisfeld, R. *J. Non-Cryst. Solids* **1985**, *74*, 395.
(7) Kaufman, V.; Avnir, D. In *Better Ceramics Through Chemistry*; Brinker, C. J., Clarck, D. E., Ulrich, D. R., Eds.; Mater. Res. Soc. Symp. Ser.; Materials Research Society: Pittsburgh, 1986; Vol. 73, p 145.
(8) Kaufman, V.; Avnir, D. *Langmuir* **1986**, *2*, 717.
(9) Kaufman, V.; Levy, D.; Avnir, D. *J. Non-Cryst. Solids* **1986**, *82*, 103.
(10) Levy, D.; Avnir, D. *J. Phys. Chem.* **1988**, *92*, 4734.
(11) MacKenzie, J. D.; Pope, E. J. A. *MRS Bull.* **1987**, *12*, 29.
(12) (a) Tani, T.; Namikawa, H.; Arai, K.; Makashima, A. *J. Appl. Phys.* **1985**, *58*, 9. (b) Makishima, A.; Tani, T. *J. Am. Ceram. Soc.* **1986**, *69*, C-72.
(13) Bertelson, R. C. Photochromism. In *Techniques of Chemistry*; Brown, G. H., Ed.; Wiley-Interscience: New York, 1971; Vol. III, Chapter VII, p 100.
(14) Pouxviel, J. C.; Boilot, J. P. *J. Mater Sci.*, in press.
(15) Pouxviel, J. C.; Boilot, J. P.; Lecomte, A.; Dauger, A. *J. Phys. (Paris)* **1987**, *48*, 921.
(16) Boilot, J. P.; Pouxviel, J. C.; Dauger, A.; Wright, A. In *Better Ceramics Through Chemistry III*; Brinker, C. J., Clark, D. E., Ulrich, D. R., Eds.; MRS Symp. Proc. Vol. 121; Materials Research Society: Pittsburgh, 1988; pp 121–126.